

## Depinning Transition in Material Failure

L. Ponson<sup>1,2</sup>, G. Cordeiro<sup>2,3</sup>

<sup>1</sup>*Division of Engineering and Applied Science, California Institute of Technology,  
Pasadena, CA 91125, USA*

<sup>2</sup>*Programa de Engenharia Civil, COPPE/UFRJ, Rio de Janeiro, Brazil*

<sup>3</sup>*Laboratorio de Engenharia Civil, UENF, Campos, Brazil*

### 1. Introduction

Failure of inhomogeneous materials has been a very active field of research during the last decades (see Ref. [1] for a recent review). A great research effort in this field has been dedicated to the study of fluctuations: Fluctuations of velocity around the average motion of cracks when the studies were devoted to their highly intermittent dynamics [2–5], or variations to a straight trajectory when the works were dedicated to the rough geometry of fracture surfaces [6–8]. In both cases, these fluctuations were shown to display remarkably robust properties suggesting that crack propagation in disordered systems could be described on a general manner by relatively simple statistical models able to capture the competition between the two antagonist effects occurring during failure of inhomogeneous materials: Disorder and elasticity. Very recently, main statistical features of fluctuations of both trajectory and velocity for cracks propagating in brittle materials were captured by stochastic models of elastic lines driven in random media [9, 10] that mimic the motion of cracks through the microstructural disorder of materials. However, the relevance of this theoretical framework for fracture problems is still a matter of debate: On the one hand, the ability of these models to describe the average behavior of the crack such as its mean velocity, or the critical external loading at failure, more interesting from a mechanical or an engineering point of view, is still an open question. On the other hand, a direct experimental observation of the critical dynamic transition from a crack pinned by the heterogeneities of the material ( $v = 0$ ) to a propagating crack ( $v > 0$ ), as predicted by this theory at the onset of material failure (driving force  $G = G_c$ ) is still lacking. The investigation of this depinning transition on an experimental example is the central point of this study. The variations of the average crack velocity with the external driving force corresponding to the elastic energy release rate  $G$  as fracture occurs [11] are measured for a brittle rock. They are shown to exhibit two distinct regimes. Below a critical threshold  $G_c$ , the crack

velocity is well described by an exponential law  $v \sim e^{-\frac{c}{G-\langle \Gamma \rangle}}$ , characteristic of a subcritical propagation, while for larger values of the external loading  $G > G_c$ , the velocity evolves as a power law  $v \sim (G - G_c)^\theta$  with  $\theta = 0.80 \pm 0.15$ . This behavior is fully captured by a stochastic model rigorously derived from Fracture Mechanics and extended to inhomogeneous systems where crack propagation is analogous to the motion of an elastic line driven in a random medium.

## 2. Experiment

### 2.1. Choice of the material and experimental method

Sandstone is chosen as an archetype of heterogeneous elastic materials. A Botucatu sandstone, extracted in the central region of Brazil, has been used for the experiments. It is made of quartz grains with a diameter  $d = 230 \mu\text{m} \pm 30 \mu\text{m}$  and a porosity  $\phi = 18 \pm 2 \%$ , that results in highly inhomogeneous mechanical properties at the grain scale. This South American rock is consolidated thanks to iron oxide cement providing to the rock a red coloration. As a result, its fracture energy  $G_c \approx 140 \text{ Jm}^{-2}$  as measured in the following is relatively high compared to other sandstones [12]. Its intrinsic tensile strength measured by splitting cylinders submitted to uniaxial compression [13] is found to be  $\sigma_Y = 80 \text{ MPa} \pm 10 \text{ MPa}$  while its Young's modulus is found to be  $E = 25 \pm 1 \text{ GPa}$ . This leads to an estimate of the size of the process zone next to the crack tip where damage and dissipative processes are localized  $\ell_{PZ} = \frac{\pi G_c E}{8 \sigma_Y^2} \approx 200 \mu\text{m}$  [14]. The comparison

with the grain size  $d > \ell_{PZ}$  suggests that crack propagation in the Botucatu rock can almost be assimilated to the motion of a crack in an ideal brittle material where the quartz grains play the role of the basic microstructural feature. A new experimental setup has been developed in order to measure variations of crack velocity from slow to very fast propagation in brittle materials. Contrary to the torsion tests classically used to measure the  $v(G)$  curves in rocks [12, 15], the Tapered Double Cantilever Beam specimens as used in the experiments (Fig. 1(a)) result in a slight and controlled acceleration of the crack that is produced by the tapered shape of the samples. As a consequence, it is possible to measure crack velocities up to  $v \approx 1 \text{ ms}^{-1}$  not achieved by classical fracture tests. In addition, the external tensile loading produces crack fronts with macroscopically straight shapes, so that the local velocity and the energy release rate are roughly constant along the crack line. This will allow for the derivation of a rather simple model to interpret the experiments. Finally, a controlled crack propagation along a straight trajectory has been obtained in the specimens without the help of lateral guide grooves, known to produce a large scattering of the experimental  $v(G)$  curves [15].

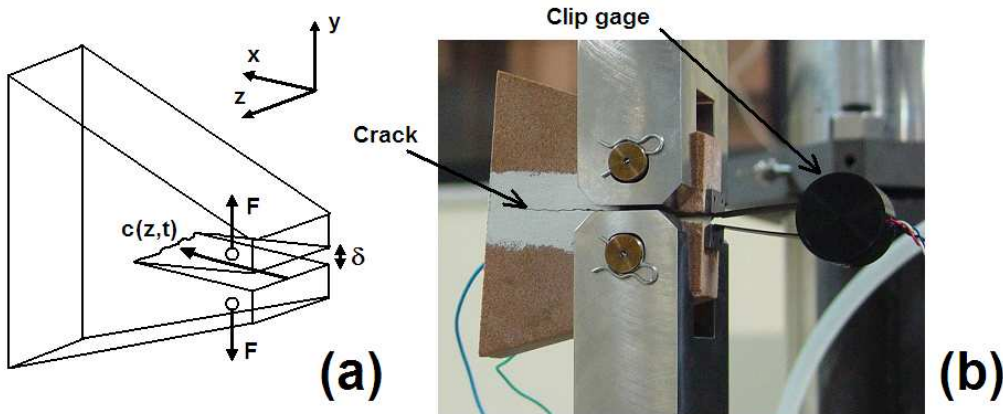


Figure 1: Experimental setup. (a) Sketch of the Tapered Double Cantilever Beam geometry; (b) picture of the specimen during crack propagation.

An initial notch  $c_0 = 35$  mm is machined in 100 mm long samples with thickness  $e = 30$  mm. They are submitted to a uniaxial traction by increasing the displacement  $\delta F = v_{\text{ext}} t$  at constant velocity  $0.2 \mu\text{m s}^{-1} \leq v_{\text{ext}} \leq 4 \mu\text{m s}^{-1}$  between two rods previously inserted in the drilled specimens. The experiments are performed at room temperature with a humidity of  $76\% \pm 4\%$ . During the test, a force gauge measures the applied tension  $F$  while a clip gage measures the opening displacement  $\delta$  between the two lips of the crack with a precision of 100 nm (see Fig. 1(b)). A typical force-crack opening displacement curve obtained during a fracture test of a Botucatu specimen is presented in Fig. 2.

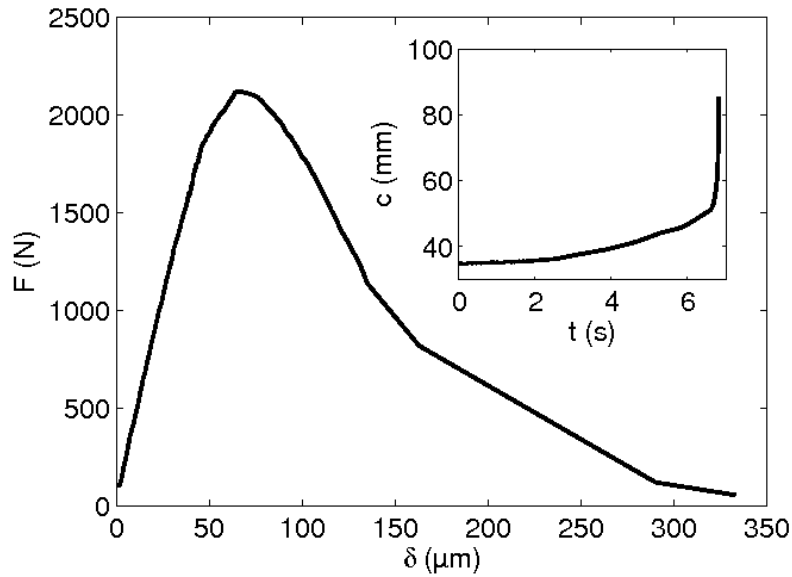


Figure 2: Mechanical behavior of the specimen. (a) Typical load-crack opening displacement curve; (b) corresponding evolution of the average position of the crack front.

The initial linear part of the curve – prior crack initiation – allows for an estimation of the Young's modulus  $E = 25 \pm 1$  GPa of the sandstone, in agreement with the value obtained from the measurement of its compressive and shear waves speed. After crack initiation, the average position of the crack front  $c = \langle c(z) \rangle_z$  is measured using Finite Element (FE) simulations of an elastic specimen in the same geometry: we run several simulations with various values of the crack length  $c$  to measure the variations of the specimen compliance  $\lambda_{\text{FE}}(c)$ . This function is then compared to the experimental compliance  $\lambda(t) = \delta/F$  in order to measure the crack length  $c(t)$  at each time step  $t$ . The variations of  $c(t)$  are represented in inset of Fig. 2. Other techniques limited to the free surface of the sample based either on image analysis of the crack motion at the surface or on the resistance measurement of a thin conductive film deposited on the sample side have led to similar, however less precise measurements of the crack length.

From the evolution of the crack length, it is now possible to measure the crack speed  $v = \frac{dc}{dt}$  as well as the driving force  $G$  imposed to the system during the test.

Using the load-displacement curve to measure the work  $\delta W$  of the tensile machine during the span  $\delta t$ , one gets  $G(t) = \delta W(t)/e[c(t+\delta t)-c(t)]$  [16]. On the other hand, the driving force is estimated independently using the relation  $G(t) = [F(t)]^2 g_{FE}[c(t)]$  where the geometrical part  $g_{FE}$  of the energy release rate is provided by the FE simulations. Both methods lead to similar results within 2 %.

## 2.2. Variations of the crack velocity with the energy release rate

The variations of the crack velocity with the driving force as observed on the sandstone specimens are represented in Fig. 3 in semi-logarithmic coordinates. Velocity measurements are achieved over almost five orders of magnitude, corresponding to a relatively small variation of the driving force. Irrespective of the external loading rate  $v_{ext}$ , the failure behavior of the rock is found to be systematically characterized by two very different regimes defining  $G_c$ . Near, but above this critical loading, a slight change in the driving force results in a strong variation in the crack velocity. This high sensibility is studied in more detail in the bottom right inset of Fig. 3, where  $v$  is plotted as a function of the net driving force  $G-G_c$  in logarithmic coordinates. The linear behavior in this representation suggests a power law variation of the crack velocity  $v \sim (G - G_c)^\theta$ . The value of  $G_c = 140 \pm 3 \text{ Jm}^{-2}$  is found to optimize this scaling relation, and leads to an exponent  $\theta = 0.80 \pm 0.15$  where the error bars are calculated from the variations measured from sample to sample. The variations of velocity at low driving forces  $G < G_c$  are now studied. Contrary to the previous regime, slow crack propagation in rocks has been largely investigated and shown to depend crucially on the

temperature [12, 15]. Analytical forms as  $v \sim e^{\frac{E^*}{k_B T}} G^{n/2}$  [17] or  $v \sim e^{\frac{E_0 - bG}{k_B T}}$  [18] are usually used to describe the experimental data. Both formulas reproduce correctly the measurements reported here as far as  $G < 120 \text{ Jm}^{-2}$ . The first one, largely used because of its rather simple and compact form characterised by one subcritical crack growth index, leads to  $n \simeq 34$  that compares well with the other experimental findings for sandstone [12]. The second formula leads to  $b \simeq 0.68 \cdot 10^{-20} \text{ m}^2$  which is also in agreement with the other measurements made on rocks with a similar microstructure [15]. This last description is based on the Arrhenius

law  $v \sim e^{\frac{E_a}{k_B T}}$  where the activation energy  $E_a = E_0 - b G$  represents the typical barrier along the energy landscape of the system tilted by the external force  $G$ . Resulting in high tensile forces on the interatomic bonds next to the crack tip, a large driving force  $G$  favors naturally the thermal activated processes leading to their rupture, as e.g. thermal stress fluctuations [19] and chemical reactions [20]. However, this theoretical approach supposes that the typical energy barrier remains independent of the geometry of the crack front. This assumption is perfectly fair as far as one considers the motion of a crack tip in a 2D medium, but in the more realistic situation of a 3D inhomogeneous material, the crack line can take advantage of its elasticity to deform and explore an energy landscape rather

different from the raw fluctuations produced by the material heterogeneities. In this context, one can show that  $E_a \sim \frac{1}{G - \langle \Gamma \rangle}$  as justified in the next section.

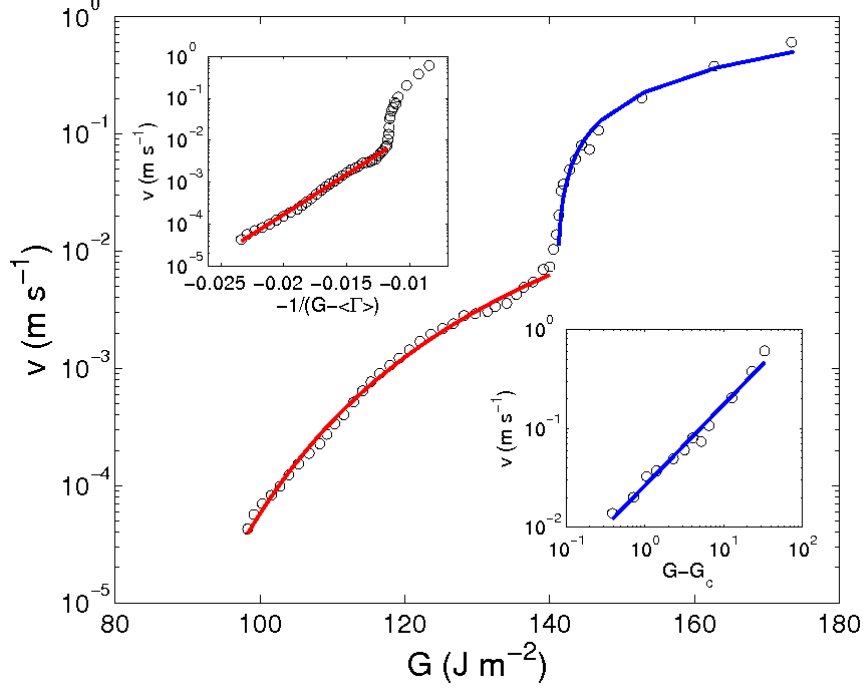


Figure 3: Average dynamics of a crack propagating in Botucatu sandstone. The variations of the crack velocity are plotted on logarithmic scale with respect to the external loading. The subcritical regime  $G < G_c$  with  $G_c = 140 \text{ J m}^{-2}$  is studied in

the top-left inset. Solid line corresponds to the best fit of the data in  $v \sim e^{\frac{c}{G - \langle \Gamma \rangle}}$  obtained for  $\langle \Gamma \rangle = 63 \text{ J m}^{-2}$ . Bottom right inset shows the velocity variations with the net loading  $G - G_c$  in a logarithm representation for  $G > G_c$ . Straight line corresponds to a power law fit with exponent  $\theta = 0.81$ .

The Arrhenius law  $v \sim e^{\frac{E_a}{k_B T}}$  provides then a good description of the experimental data for the full subcritical regime  $G < G_c$  as shown in Fig. 3. The upper left inset represents the best fit obtained for  $\langle \Gamma \rangle = 63 \pm 5 \text{ J m}^{-2}$ .

### 3. Discussion

The observation of two very different regimes with an exponential variation of  $v$  with the external loading for  $G < G_c$  and a power law behavior for  $G > G_c$  reveals a fundamental aspect of the dynamics of cracks propagating in brittle inhomogeneous media. Let's derive an equation of motion for the crack to understand more quantitatively this behavior. As a starting point, we assume that the local velocity  $v(M)$  of a point  $M$  along the crack front is proportional to the excess of energy  $G(M) - \Gamma(M)$  locally released by the system where  $\Gamma$  refers to the local fracture energy. This corresponds to a damped dynamics where the inertial effects are neglected. In a disordered material such as sandstone, the fracture energy can be described as a stochastic field  $\Gamma(M) = \langle \Gamma \rangle + \delta\Gamma \eta(M)$

where  $\eta$  is a short range correlated random term with zero mean value and unit second order moment. The heterogeneities of the material induce perturbations of the crack front – parallel in average to the  $z$ -axis and propagating along the  $x$ -axis – both in the mean fracture plane ( $x, z$ ) (in-plane perturbations  $c(z, t) - \langle c(z, t) \rangle_z$ ) and in the perpendicular direction  $y$  (out-of-plane perturbations  $h(z, t)$ ). They in turn lead to variations in the local value of the external driving force  $G(M)$ . Interestingly, for small perturbations,  $G(M)$  is only depending on the in-plane deviations of the crack front [22, 23], and is given

$$\text{by } G(z, t) = G + \frac{G}{\pi} \int \frac{c(z', t) - c(z, t)}{(z' - z)^2} dz' \quad [24] \text{ where } G \text{ refers to the macroscopic}$$

driving force applied by the tensile machine to the specimen. Using the previous expressions of the local driving force and material fracture energy, one gets the following equation of motion for a 2D crack front propagating in a 3D brittle inhomogeneous material

$$\frac{\partial c(z, t)}{\partial t} = G + \frac{G}{\pi} \int \frac{c(z', t) - c(z, t)}{(z' - z)^2} dz' + \delta\Gamma \eta(c, h, z). \quad (1)$$

As the out-of-plane perturbations  $h$  behave independently of  $c$ , the stochastic term in this equation is analogous to a 2D random potential depending only on  $c$  and  $z$ . Therefore, the crack motion is described by an equation of pinning/depinning of an elastic line driven in a random medium comparable to those proposed in the context of interfacial cracks propagating in inhomogeneous weak planes [25, 26]: if the driving force  $G$  exceeds a given threshold

$$G_c = \langle \Gamma \rangle + \pi \langle \delta\Gamma \rangle^2 / \langle \Gamma \rangle, \quad (2)$$

the crack propagates, while the front is pinned by the material heterogeneities if  $G < G_c$  [27]. Above the threshold, the mean velocity  $v$  of the crack front is expected to scale as  $(G - G_c)\theta$  where  $\theta$  is called the velocity exponent. Ertas and Kardar have studied equation (1) using functional renormalization group technique [28]. To first order in perturbation, they find  $\theta = 0.78$ . Recent direct numerical simulations resulted in  $\theta \simeq 0.63$  [29]. As a consequence, the power law behavior measured experimentally with exponent  $\theta \simeq 0.80$  suggests that a depinning transition from a pinned to a moving crack as described in Eq. (1) occurs at  $G = G_c$ . Below the threshold at zero temperature, the external driving force is not sufficient to make the crack propagate and the crack front is pinned by the material heterogeneities. However, at room temperature, thermally activated processes can enable a subcritical propagation. In this regime, described by adding an annealed noise  $\eta_T(z, t)$  to Eq. (1), one expects also a collective motion of the line characteristic of glassy systems, and velocity variations are predicted to

follow the so-called creep law  $v \sim e^{-\left(\frac{\ell}{\pi}\right)^2 \frac{\langle \Gamma \rangle^2}{k_B T (G - \langle \Gamma \rangle)^\mu}}$  where  $\mu = 1$  for the long-range elasticity of the crack front [30, 31]. This expression, first proposed for the subcritical crack dynamics in Ref. [21] and then observed in the context of paper peeling [4], describes rather well the experimental measurements presented here over the whole range of subcritical loading  $G < G_c$ , leading to activation energies

in the range  $E_a = \left(\frac{\ell}{\pi}\right)^2 \frac{\langle \Gamma \rangle^2}{G - \langle \Gamma \rangle} \approx 0.20 - 0.35$  eV, one order of magnitude larger than the thermal energy  $k_B T$ . Interestingly, the expression of the activation energy provides an estimate of the topothesy – size of the basic feature of the crack front –  $\ell \approx 0.10$  nm, compatible with the interatomic distance. This suggests that thermally activated crack propagation and critical failure might involve processes defined at two very different length scales, atomic and grain size, respectively. Finally, let us note that using Eq. (2), the experimental values of the critical driving force  $G_c$  and the average fracture energy  $\langle \Gamma \rangle$  allow an estimation of the normalized fluctuations  $\frac{\delta \Gamma}{\langle \Gamma \rangle} = \sqrt{\frac{G_c - \langle \Gamma \rangle}{\langle \Gamma \rangle}} = 0.62 \pm 0.06$  of fracture energy in the Botucatu rock, slightly larger but comparable with an estimate of this quantity  $\sqrt{\frac{\phi}{1 - \phi}} \approx 0.5$  for an ideal porous material made of an homogeneous solid with constant fracture energy and voids, with volume fractions  $1 - \phi = 0.82$  and  $\phi = 0.18$ , respectively.

#### 4. Conclusion

The average dynamics of a crack propagating in a brittle inhomogeneous rock has been experimentally investigated. The velocity variations with the external driving force display two very different regimes: above a threshold  $G_c$ ,  $v$  evolves as a power law  $(G - G_c)^\theta$  with exponent  $\theta = 0.80 \pm 0.15$  while for  $G < G_c$ , these variations are described by an Arrhenius law  $v \sim e^{-\frac{E_a}{k_B T}}$  with typical energy barriers  $E_a \sim \frac{1}{G - \langle \Gamma \rangle}$ . This behavior can be quantitatively explained extending Fracture Mechanics to disordered systems. In this description, the resistance to failure of a material is interpreted as the critical force to depin the crack front from the material heterogeneities. Below this pinning transition, the line can also propagate, but at much smaller velocities through thermal activated processes, and the velocity variations are provided by a creep law as observed experimentally. The experimental results presented here and their theoretical interpretation open new perspectives for the prediction of macroscopic quantities of direct interest for Engineering and Applied Science. They make the link between the microstructural properties of a material and its fracture energy or the crack velocity. This bridge might help to design stronger materials with increased lifetimes.

#### Acknowledgements

The authors would like to thank A. Bindal for his help in the experiments and M. Alava, K. Bhattacharya, D. Bonamy, E. Bouchaud, J.-B. Leblond, S. Morel, A. Rosso and R. Toledo for helpful discussions. Financial support from the French Ministry of Foreign Affairs through the Lavoisier Program is acknowledged.

- [1] M.J. Alava, P.K. Nukala, S. Zapperi, Statistical models of fracture, *Adv Phys* 55 (2006) 349-476
- [2] K.J. Måløy, J. Schmittbuhl, Dynamical event during slow crack propagation, *Phys Rev Lett* 87 (2001) 105502
- [3] K.J. Måløy, S. Santucci, J. Schmittbuhl, R. Toussaint, Local waiting time fluctuations along a randomly pinned crack front, *Phys Rev Lett* 96 (2006) 045501
- [4] J. Koivisto, J. Rosti, M.J. Alava, Creep of a fracture line in paper peeling, *Phys Rev Lett* 99 (2007) 145504.
- [5] J. Davidsen, S. Stanchits, G. Dresen, Scaling and universality in rock fracture, *Phys Rev Lett* 98, (2007) 125502
- [6] E. Bouchaud, G. Lapasset, J. Planès, Fractal dimension of fractured surfaces: A universal value?, *Europhys Lett* 13, (1990) 73-79
- [7] K.J. Måløy, A. Hansen, E. L. Hinrichsen, S. Roux, Experimental measurements of the roughness of brittle cracks, *Phys Rev Lett* 68 (1992) 213-215
- [8] L. Ponson, D. Bonamy, E. Bouchaud, Two-dimensional scaling properties of experimental fracture surfaces, *Phys Rev Lett*, 96 (2006) 035506
- [9] D. Bonamy, L. Ponson, S. Prades, E. bouchaud, C. Guillot, Scaling exponents for fracture surfaces in homogeneous glass and glassy ceramics, *Phys Rev Lett* 97 (2006) 135504
- [10] D. Bonamy, S. Santucci, L. Ponson, Crackling dynamics in material failure as the signature of a self-organized dynamic phase transition, *Phys Rev Lett* 101 (2008) 045501
- [11] B. Lawn, *Fracture of brittle solids*, Cambridge University Press, Cambridge, 1993
- [12] B.K. Atkinson, Subcritical crack growth in geological materials, *J Geophys Res* 89 (1984) 4077-4114
- [13] F.L.L.B. Carneiro, A. Barcellos, Résistance à la traction des bétons, *Bulletin RILEM* 1 (1953) 97-108
- [14] G.I. Barenblatt, The mathematical theory of equilibrium cracks in brittle fracture, *Adv Appl Mech* 7 (1962) 55-129
- [15] Y. Nara, K. Kaneko, Subcritical crack growth in anisotropic rock, *Int J Rock Mech Min Sci* 42 (2005) 521-530
- [16] S. Morel, N. Dourado, G. Valentin, J. Morais, Wood: A quasi-brittle material. R-curve behavior and peak load evaluation, *Int J Frac* 131 (2005) 385-400
- [17] R.J. Charles, Static fatigue of glass II, *J Appl Phys* 29 (1959) 1554-1560
- [18] S.M. Wiederhorn, H. Johnson, A.M. Dinensand, A.H. Heuer, Fracture of glass in vacuum, *J Am Ceram Soc* 57 (1974) 336-341
- [19] S. Santucci, L. Vanel, S. Ciliberto, Subcritical statistics in rupture of fibrous materials: Experiments and models, *Phys Rev Lett* 93 (2004) 095505
- [20] S. M. Wiederhorn, Influence of water vapor on crack propagation in soda-lime glass, *J Am Ceram Soc* 50, (1967) 407-414
- [21] L. Ponson, D. Bonamy, E. Bouchaud, G. Cordeiro, R.D. Toledo, E.M.R. Fairbairn, Path and dynamics of a crack propagating in a disordered material



- under mode I loading, in: A. Carpinteri (Eds.), Proceeding FRAMCOS-6, 2007, pp. 63–67
- [22] A.B. Movchan, H. Gao, J.R. Willis, On perturbations of plane cracks, *Int J Solids Struct* 35 (1998) 3419-3453
- [23] R.C. Ball and H. Larralde, Three-dimensional stability analysis of planar straight cracks propagating quasistatically under type I loading, *Int J Frac* 71 (1995) 365-377
- [24] J.R. Rice, First-order variation in elastic fields due to variation in location of a planar crack front, *J Appl Mech* 52 (1985) 571-579
- [25] J. Schmittbuhl, S. Roux, J.P. Vilotte, K.J. Måløy, Interfacial crack pinning: effect of nonlocal interactions, *Phys Rev Lett* 74 (1995) 1787-1790
- [26] S. Ramanathan, D. Ertas, D.S. Fisher, Quasistatic crack propagation in heterogeneous media, *Phys Rev Lett* 79 (1997) 873-876
- [27] A.L. Barabási and H.E. Stanley, *Fractal concepts in surface growth*, Cambridge University Press, Cambridge, 1995
- [28] D. Ertas, M. Kardar, Critical dynamics of contact line depinning, *Phys. Rev. E*, 49 (1994) R2532
- [29] O. Duemmer, W. Krauth, Depinning exponents of the driven long-range elastic string, *J. Stat. Mech.* 1 (2007) 01019
- [30] M.V. Feigelman, V.B. Geshkenbein, A.I. Larkin, V.M. Vinokur, Theory of collective flux creep, *Phys Rev Lett* 63 (1989) 2303-2306
- [31] A.B. Kolton, A. Rosso, T. Giamarchi, Creep motion of an elastic string in a random potential, *Phys. Rev. Lett.* 94 (2005) 047002  
135-155